C_{60}: Interacting electrons on a spherical molecule

Ganpathy N. Murthy
Department of Physics, Boston University, Boston, Massachusetts 02215

Assa Auerbach
Department of Physics, Boston University, Boston, Massachusetts 02215
and Department of Physics, Technion-IIT, Haifa 32000, Israel
(Received 30 October 1991)

We study a simplified model of C_{60}, where the π electrons move freely on the surface of a sphere. The total energy in the presence of an adjustable repulsive interaction is computed by first- and second-order perturbation theory. The second-order results yield an effective attraction (pair binding) between electrons which are added above a closed angular-momentum shell. For different regimes of interaction parameters, we find an $L=0$ singlet and an $L=1$ triplet ground state. Pair binding occurs at larger couplings for longer-range interactions. We estimate the third-order corrections, and define the region where the second-order predictions are expected to hold. The relevance of this model to superconductivity and ferromagnetism in doped fullerenes is discussed.

I. INTRODUCTION

For many years theorists have been intrigued by the possibility of pair binding and superconductivity in electronic systems with purely repulsive interactions. Superconductivity in strongly correlated metals (e.g., heavy-electron compounds and high-T_c cuprates) suggests that large repulsive interactions can sometimes be transformed into an effective attraction between quasiparticles. This is quite distinct from the attraction induced by the electron-phonon mechanisms, which so successfully accounts for many superconductors. In the electron-phonon system, there is a fundamental separation of time scales between the motion of the light electrons and heavier ions. This produces an effective *retarded* attraction between electrons, which can overcome the larger but instantaneous Coulomb repulsion. Superconductivity in purely electronic systems is intriguing because such a separation in time scales is not obviously present, and the mechanisms of overcoming the instantaneous repulsions is harder to understand.

Following the recent discovery of superconductivity in alkali-metal-doped fullerites[1] (X_3C_{60}, X=K,Rb), Chakravarty and Kivelson (CK) have proposed that electron-electron interactions can contribute substantially to the pairing mechanism on the C_{60} molecules.[2] Each isolated molecule is a system of 60 π electrons and 180 σ electrons, all interacting with each other. The pair energy of two extra electrons added to an N-electron system is defined as[3]

$$\Delta_N \equiv E_{N+2} - 2E_{N+1} + E_N \ . \tag{1.1}$$

Here E are the ground-state energies. *Pair binding* ($\Delta<0$) occurs when two added electrons on one molecule have lower energy than when they occupy two separate molecules. The *binding energy* of the pair is defined as $-\Delta$. Exact numerical solutions of the Hubbard and t-J models in one- and two-dimensional clusters[4] have shown that pair binding often occurs in these repulsively interacting systems.

Pair binding in conjunction with intermolecular hopping processes has been proposed by CK as an explanation of the relatively high-temperature superconductivity in the fullerenes. CK considered only the π electrons interacting via a Hubbard interaction. The neglected shells and crystal environment are assumed to produce sufficient screening to convert the long-range Coulomb repulsion into the short-range Hubbard repulsion. CK consider the Hubbard model on the tight-binding truncated icosahedral lattice, with hopping energy t and on-site repulsion U. Since X_3C_{60} has an average of 63 π electrons per C_{60} molecule, the relevant Δ_N is that of $N=62$. Δ is computed up to second-order perturbation theory in U/t. For $U \geq 3t$, Δ truncated at second order becomes negative in the singlet channel.

In this paper we address several questions which are inspired by the aforementioned work: (i) Is the underlying lattice potential essential for pair binding? (ii) What are the effects of long-range Coulomb interactions? (iii) In what cases can one trust the extrapolated results of second-order perturbation theory? We will explain in full detail the methods and results that were presented briefly in an earlier publication.[5]

We begin by removing the lattice potential entirely and consider a system of electrons moving freely on the surface of a sphere. The electrons interact by a two-body potential which is parametrized by its strength g and range α. $\alpha=0$ corresponds to a short-range interaction $\alpha=1$ to the unscreened $1/r$ Coulomb interaction. Thus the parameter $\alpha<1$ simulates the screening of the long-range tails of the interaction, although "range" is hard to define on a finite sphere. We emphasize that α does not describe the full dynamical screening effects. A complete treatment of screening is very complicated, with contributions coming from neglected shells on a single C_{60} mol-

ecule as well as from image charges on neighboring C_{60} molecules in the fullerene lattice.

We consider a system of π electrons with an effective interaction characterized by (g,α). We do not attempt an *ab initio* approach. Rather, our goal is to examine general dependences of the pair energy on simple physical parameters. Presumably, the trends which are found to be robust will survive in a more detailed model.

We use perturbation theory to compute the pair energy Δ for the case of two ("conduction") electrons in the lowest open angular-momentum shell. First-order perturbation theory always gives a non-negative contribution to Δ. Second-order perturbation theory gives a positive or negative contribution to Δ depending on the total angular momentum. We find that the singlet channel $L=0$ (where L is the orbital angular momentum) has a negative second-order contribution in all the cases we have studied. Often the triplet ($L=1$) channel also has a negative second-order term. If we neglect all higher-order contributions, $\Delta(L)$ becomes negative beyond a certain interaction strength $g^{\text{pair}}(L)$. Naturally, we must investigate the validity of our truncation.

As mentioned before, the exact diagonalizations of finite Hubbard and t-J clusters in one and two dimensions[4] demonstrate the existence of pair binding at moderate and large couplings. Furthermore, it appears that the existence of pair binding is correlated with the negativity of the second-order coefficient of Δ. Unfortunately, exact solutions for the longer-range interactions are not yet available.

To address this problem, we must estimate the characteristic magnitude of the coupling g^{pert}, above which the higher order terms can be large. At g^{pair} the first- and second-order energies are equal in magnitude. At first thought it might seem natural that the third-order term should also be of the same magnitude as the first two and thus $g^{\text{pert}}=g^{\text{pair}}$. This would lead us to conclude that we *cannot* predict pair binding since it would always occur where third- and higher-order terms are large. However, the first-order energy has a different status than the rest of the terms: It does not involve energy denominators. The second- and higher-order terms, however, depend on the single-particle energy levels. g^{pert} therefore is better estimated by $g^{\text{pert}}\approx|E^{(2)}/E^{(3)}|$, where $E^{(2)}$ and $E^{(3)}$ are the second- and third-order coefficients of the energy. Strictly speaking, the radius of convergence of the perturbation series is a property not of the first few terms of a series, but of infinitely many terms. Therefore g^{pert} as defined above is only a crude guideline. If $g^{\text{pair}}<g^{\text{pert}}$, the confidence in the occurrence of pair binding is large. If not, perturbation theory cannot be trusted to predict pair binding. Therefore we have invested some effort in estimating the third-order term $E^{(3)}$ and g^{pert}. In the process we will make a simplifying assumption about the behavior of the matrix elements in the perturbation-series sums. The assumption will be stated later and can be justified *a posteriori*.

The results can be broadly summarized as follows: Pair binding occurs with high confidence for highly screened interactions ($\alpha<0.1$). In this regime pair binding in the triplet ($L=1$) channel occurs before pair binding in the singlet ($L=0$) channel. Indeed, triplet pair binding occurs at arbitrarily small values of g for the δ-function potential. If our parameters and filling numbers are realized in a real material, this would lead to a novel ferromagnetic superconductor.

As a result of these calculations, we shall be able to answer the three questions posed above. The phenomenon of pair binding does not require a strong lattice potential, since we are able to get it in our free-electron model. The effect of long-range interactions is to increase g^{pair} and reduce the radius of convergence of perturbation theory, g^{pert}, so that the shorter the range, the more confidence we have in the existence of pair binding.

The paper is organized as follows: In Sec. II we set up the Hamiltonian and define the potential. Section III will describe the standard perturbation theory. In Sec. IV we derive an independent diagrammatic method to compute Δ. In Sec. V we estimate the third-order contribution and range of couplings for which second-order perturbation theory is expected to be valid. The results are presented in detail in Sec. VI. In Sec. VII we present an effective negative-U Hubbard model based on our results which could lead to superconductivity in doped fullerenes. Some tedious formulas from Sec. V are relegated to the Appendix.

II. MODEL

A. Zeroth order

Our zeroth-order Hamiltonian is that of noninteracting electrons of mass m^* moving on the surface of a sphere of radius R. The single-particle eigenstates are

$$|lms\rangle = Y_{lm}(\hat{\Omega})\chi_s \ , \tag{2.1}$$

$$l=0,1,\ldots, \quad m=-l,-l+1,\ldots,l \ , \quad s=\uparrow,\downarrow \ ,$$

where Y_{lm} is a spherical harmonic, $\hat{\Omega}$ is a unit vector, and χ_s is the spin-$\frac{1}{2}$ wave function. In second-quantized notation, the Hamiltonian is

$$H_0=\sum_{l=0}^{l_{\max}}\sum_{m=-l}^{l}\sum_{s=\uparrow\downarrow}\varepsilon_l c^{\dagger}_{lms}c_{lms} \ , \tag{2.2}$$

$$\varepsilon_l=e_0 l(l+1) \ ,$$

where $c^{\dagger}_{lms}$ creates an electron in the state (2.1) and $e_0=\hbar^2/(2m^*R^2)$ is the unit of kinetic energy. In (2.2) we discard the radial degrees of freedom, assuming that the electrons are confined by the ions to a narrow shell close to radius R. In Fig. 1(a) we show the spectrum of H_0 up to $l_{\max}=6$. It is instructive to compare this spectrum with that of the tight-binding model on the truncated icosahedron (TI) lattice of C_{60} (Ref. 6) given by

$$H_0^{\text{TI}}=-t\sum_{s,\langle ij\rangle}c^{\dagger}_{is}c_{js} \ , \tag{2.3}$$

where $\langle ij\rangle$ denote nearest-neighbor bonds on the TI lattice. The spectrum of H_0^{TI} from Ref. 2 is plotted in Fig.

1(b) where the energy scales of the two models are approximately matched. There is an obvious correspondence between the TI multiplets and angular-momentum shells, although the effects of the lattice are also apparent. The lattice splits the $(2l+1)$-fold degeneracies into smaller multiplets. As depicted in Fig. 1(b), the $l=5$ multiplet is broken into three sets, and the Fermi energy of the 60-electron system lies between the fivefold and threefold multiplets.[2]

The single-particle degeneracy of the highest occupied multiplet translates into a much larger degeneracy for the ground state of the partially filled system. Ground-state degeneracy complicates perturbation theory. Fortunately, we can use symmetry to reduce the number of virtual states we have to consider. An obvious advantage of the spherical model is that the continuous-rotation group has simpler representations than the discrete icosahedral point group.

The physical justification for ignoring the lattice potential is that we are primarily interested in the effects of Coulomb interactions which are as large as, or larger than, the lattice-induced gaps. In our model the degeneracy of the ground state is lifted by the Coulomb interactions. For the TI model with strong interactions, one might worry about large higher-order corrections to second-order perturbation theory. Those would be produced by the small lattice gaps which enter as energy denominators in the perturbation series.

The cutoff angular moment $l_{\max}$ limits the number of single-particle states (including spin degeneracy) to $2(l_{\max}+1)^2$. This means that fluctuations at scales smaller than $r_{\min}=2/(l_{\max}+1)$ are not included. Physically, the discarded states with energy higher than $e_0 l_{\max}(l_{\max}+1)$ are the extended (ionized) states which do not couple strongly to the electrons on the sphere.

B. Interactions

The two-body interactions between electrons on the sphere are parametrized by two dimensionless variables g and α, the strength and range of the interactions, respectively:

$$\hat{V}^{\alpha}=\tfrac{1}{2}\int d\hat{\Omega}_1 d\hat{\Omega}_2 v^{\alpha}(\hat{\Omega}_1-\Omega_2):\rho(\hat{\Omega}_1)\rho(\hat{\Omega}_2):\,, \qquad (2.4)$$

$$v^{\alpha}=g2\pi r_{\min}e_0 \times \sum_{L,M,s,s'}\left[\frac{2}{r_{\min}(2L+1)}\right]^{\alpha} Y^{*}_{LM}(\hat{\Omega}_1)Y_{LM}(\hat{\Omega}_2)\,,$$

$\rho=\sum_s \psi_s^{\dagger}\psi_s$ is the density operator, where $\psi_s^{\dagger}=\sum_{l,m} Y_{lm}(\hat{\Omega})c_{lms}^{\dagger}$. The strength of the potential is

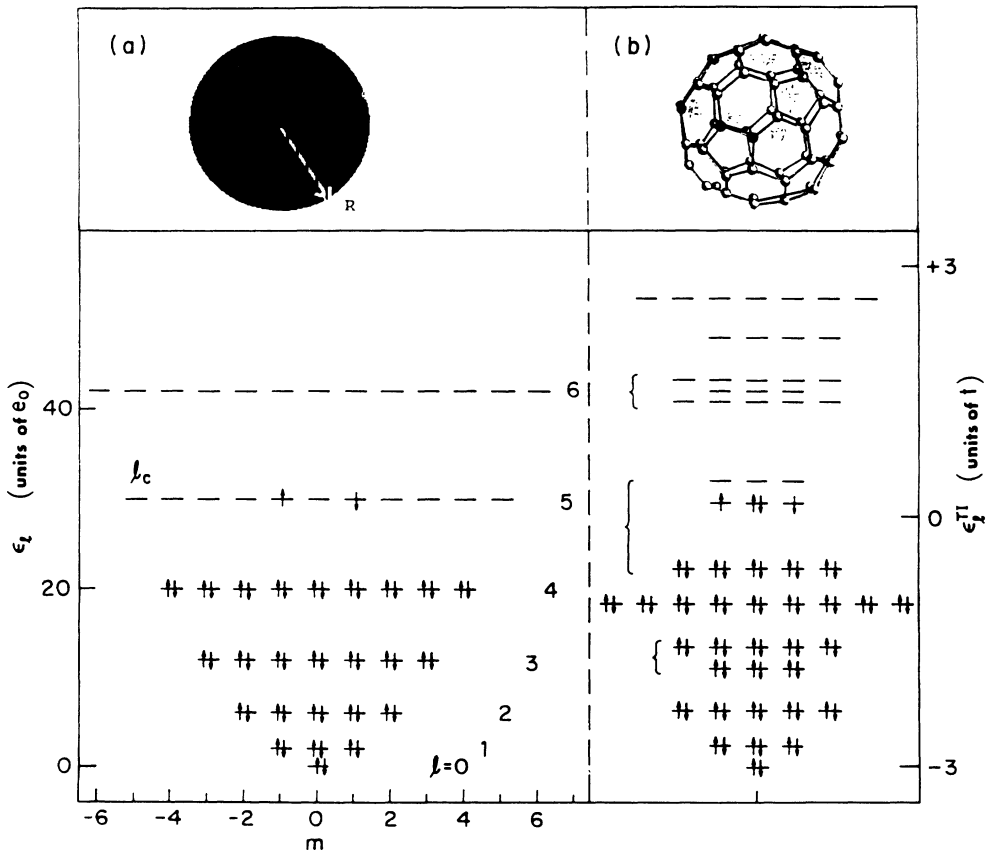

FIG. 1. (a) Spectra of noninteracting electrons on a sphere [Eq. (2.2)] with $l_c=5$ and $l_{\max}=6$. We show the occupied states in one of the degenerate ground states of the 52-electron system. (b) The spectrum of the noninteracting tight-binding model (Ref. 6) on the truncated icosahedron (TI) lattice [Eq. (2.3)]. The lattice is depicted on top. The occupied states of a 63-electron ground state are shown.

given by $g=e^2/(\epsilon R e_0)$, where ϵ is the short-distance dielectric constant. The power-law tail of $v(r)$ decreases with α. $0\le\alpha\le 1$ interpolates smoothly between the localized δ function and long-range Coulomb potential:

$$v^{\alpha=0}=g2\pi r_{\min}e_0\delta(\hat{\Omega}_1-\hat{\Omega}_2)\ ,$$
$$v^{\alpha=1}=\frac{ge_0}{|\hat{\Omega}_1-\hat{\Omega}_2|}\ . \tag{2.5}$$

To illustrate the effective range of interactions, we convolute the potential with a Gaussian of width $r_{\min}$. Also, we truncate the interaction momenta at $2l_{\max}$, which is the largest momentum that can be exchanged between particles with $l\le l_{\max}$. In other words, we consider the function

$$\tilde{v}^{\alpha}(\theta)=\frac{r_{\min}}{\sqrt{\pi}}\int d\theta'\, e^{-[(\theta-\theta')/r_{\min}]^2}\times\sum_{L=0}^{2l_{\max}}\left[\frac{2L+1}{l_{\max}+1}\right]^{1-\alpha}P_L(\cos\theta')\ , \tag{2.6}$$

where P_L are Legendre polynomials. Figure 2 demonstrates the dependence of $\tilde{v}^{\alpha}$ on α for $l_{\max}=6$.

We can compare the interactions in the $\alpha=0$ limit to the Hubbard interaction on the TI lattice of Eq. (2.3):

$$\hat{U}=U\sum_i c_{i\uparrow}^{\dagger}c_{i\uparrow}c_{i\downarrow}^{\dagger}c_{i\downarrow}\ . \tag{2.7}$$

The Hubbard interaction is localized on the atomic orbitals. In our continuous model, we choose to keep the averaged interaction over an area of radius $r_{\min}$, independent of α. The analogous interaction parameter to the Hubbard U is $\tilde{U}$:

$$\tilde{U}\equiv\frac{1}{\pi r_{\min}^2}\int d^2\theta\, v^{\alpha=0}=\frac{1}{\pi r_{\min}^2}\int_{|\theta|<r_{\min}}d^2\theta\, v^{\alpha=1}=\frac{2ge_0}{r_{\min}}\ . \tag{2.8}$$

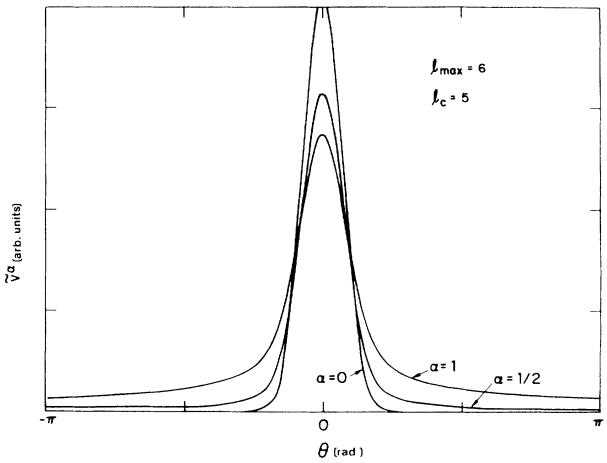

FIG. 2. Truncated interaction potential of Eq. (2.6). θ is the angular distance on the sphere, and α parametrizes the range of the interaction.

The analogous parameter to the tight-binding hopping t is deduced by comparing the bandwidths of Eqs. (2.2) and (2.3). For the (TI) lattice, the bandwidth is $W\approx 5t$. Here we choose the upper band edge $\tilde{W}$ to be half-way between the $l_{\max}$ and $l_{\max}+1$ shells. Thus

$$\tilde{W}=5\tilde{t}=(l_{\max}+1)^2e_0\ . \tag{2.9}$$

By (2.8) and (2.9) and by the definition of $r_{\max}$, we find that

$$\frac{\tilde{U}}{\tilde{t}}=\frac{5g}{(l_{\max}+1)}\ . \tag{2.10}$$

In the single-particle basis, the two-body interactions $\hat{V}^{\alpha}$ of (2.4) have a convenient parametrization

$$\hat{V}^{\alpha}=\tfrac{1}{2}v^{\alpha}_{lml'm'\lambda'\mu'\lambda\mu}c^{\dagger}_{l'm's}c^{\dagger}_{\lambda'\mu'\alpha}c_{\lambda\mu\sigma}c_{lms}\ , \tag{2.11}$$

where summation of repeated indices is assumed. The matrix elements of the potential are given by the formula

$$v^{\alpha}=g2\pi r_{\min}\sum_L\left[\frac{2}{r_{\min}(2L+1)}\right]^{\alpha}(-1)^{m'+\mu}C^{Ll l'}_{Mm-m'}C^{L\lambda\lambda'}_{-M\mu-\mu'}\ . \tag{2.12}$$

The vertices C are given by

$$C^{Ll l'}_{Mm-m'}=\int d\Omega\, Y_{LM}(\Omega)Y_{lm}(\Omega)Y_{l'-m'}(\Omega)=\delta_{M+m-m',0}\left[\frac{(2L+1)(2l+1)(2l'+1)}{4\pi}\right]^{1/2}\begin{pmatrix}L & l & l'\\ M & m & -m'\end{pmatrix}\begin{pmatrix}L & l & l'\\ 0 & 0 & 0\end{pmatrix}\ . \tag{2.13}$$

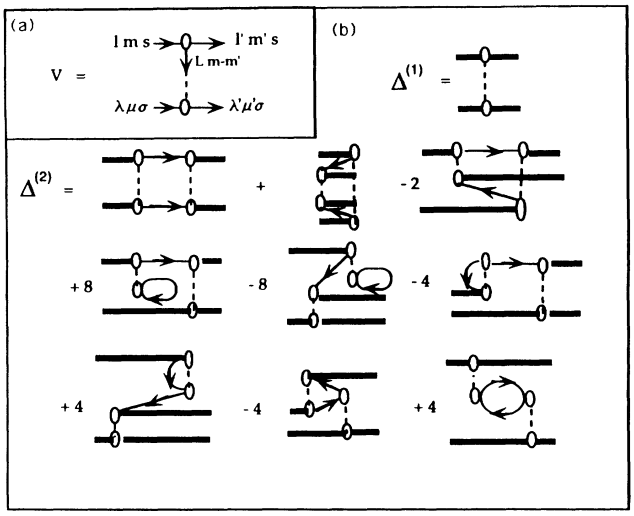

FIG. 3. (a) Diagrammatic representation of the interaction of Eq. (5). Each vertex represents a factor of C. (b) First- and second-order diagrams for the pair-binding energy with their combinatorial factors. Right (left and vertically) pointing arrows denote unoccupied (occupied) states of the $n=0$ system. Thick lines denote conduction-electron states. Rules for evaluating the diagrams are outlined in Sec. IV.

The diagrammatic notation for the interaction v^{α} is depicted in Fig. 3(a). The six-argument forms denote standard $3j$ symbols which are defined in Ref. 7.

III. PERTURBATION EXPANSION OF THE ENERGY

In the following we limit our discussion to the case of l_c filled shells, $l=0,\ldots,l_c-1$, and $n=0,1,2$ additional electrons in the first open "conduction" shell, $l=l_c$. The total number of electrons is $N+n=2l_c^2+n$. The energies E_{N+n} are computed perturbatively in g. The interaction commutes with the total-angular-moment and total-spin operators. Thus the exact eigenstates are labeled by L, L^z, and S, and S^z. The energies are independent of (L^z,S^z), which we fix to be (0,0), $(0,+\frac{1}{2})$, and (0,0) for $n=0$, 1, and 2, respectively. This lifts the degeneracies of the noninteracting ground states of the $n=0$ and 1 systems, but leaves a manifold of $2l_c+1$ degenerate ground states for the $n=2$ system. The states Φ_n are given by

$$\Phi_0=|N\rangle\ ,\quad \Phi_1=c^{\dagger}_{l_c 0\uparrow}|N\rangle\ ,$$
$$\Phi_2^m=c^{\dagger}_{l_c -m\uparrow}c^{\dagger}_{l_c m\downarrow}|N\rangle\ , \tag{3.1}$$

where $|N\rangle$ is the closed-shell state. In Fig. 1(a) we depict the occupied states of the ground state $\Phi^{m=1}_{N+2}$, where $N=50$ electrons.

The perturbation expansion of the energy is given by the standard formula

$$E_{N+n}(m,m';g)=\sum_{k=0}^{\infty} g^k E^{(k)}_{N+n}(m,m')\ ,$$
$$gE^{(1)}=\langle\Phi_n^m|\hat{V}|\Phi_n^{m'}\rangle\ ,$$
$$g^2E^{(2)}=\left\langle\Phi_n^m\left|\hat{V}\frac{1-\mathcal{P}_0}{E^{(0)}-H_0}\hat{V}\right|\Phi_n^{m'}\right\rangle\ , \tag{3.2}$$
$$g^3E^{(3)}=\left\langle\Phi_n^m\left|\hat{V}\left[\frac{1-\mathcal{P}_0}{E^{(0)}-H_0}\hat{V}\right]^2\right|\Phi_n^{m'}\right\rangle$$
$$-gE^{(1)}\left\langle\Phi_n^m\left|\hat{V}\frac{1-\mathcal{P}_0}{(E^{(0)}-H_0)^2}\hat{V}\right|\Phi_n^{m'}\right\rangle\ ,$$

where $E^{(0)}$ is the energy of (2.1) and $\mathcal{P}_0$ projects onto the ground state or ground-state manifold (for the case of $n=2$). Since the H_0 and $\hat{V}$ are rotationally invariant, we can diagonalize the terms in the total L and S representation. For the $n=2$ case, the total spin S of the ground-state manifold can be either a singlet ($S=0$) or a triplet ($S=1$). For the total wave function to be antisymmetric, we *must have* $L+S$ *even*. Therefore S (L) is completely determined by these conditions, and the available quantum numbers of the ground-state multiplet are $(L,S)=(0,0)$, (1,1), (2.0), etc. This allows us to simultaneously diagonalize all the terms in the perturbation series (3.1) by the Clebsch-Gordan transformation[7] as

$$\sum_{m,m'}(L0|l_c-m,l_cm)E^{(k)}_{N+2}(m,m')(l_cm'l_c-m'|0L')$$
$$=\delta_{LL'}E^{(k)}_{N+2}(L)\ . \tag{3.3}$$

The cases of additional conduction electrons in the open shell involve couplings of three and more angular momenta. These cases will not be treated in this paper.

By (3.2) the first-order energies are

$$E^{(1)}_{N+n}=\sum_{a,b}^{\text{occ}}\langle a,b|\hat{V}|b,a\rangle\ ,\quad n=0,1\ ,$$
$$E^{(1)}_{N+2}(m,m')=\sum_{a,b}^{\text{occ}(m)}\sum_{a',b'}^{\text{occ}(m')}\langle a,b|\hat{V}|b',a'\rangle\ . \tag{3.4}$$

The sums $\sum_{a,b}^{\text{occ}(m)}$ are over all occupied states in Φ_n^m. These first-order energies can be quite large. As can be seen from Eq. (3.2), they appear in third and higher orders and can vitiate the perturbation theory. To avoid this problem, we measure all energies from the ground-state energy including the first-order correction. In other words, we decompose the Hamiltonian as

$$H=H_0+\langle n,L|\hat{V}|n,L\rangle+(\hat{V}-\langle n,L|\hat{V}|n,L\rangle)$$
$$=H_0'+\hat{V}'\ , \tag{3.5}$$

where $\langle n,L|\hat{V}|n,L\rangle$ is the first-order correction to the energy of the ground state with n added particles and total angular momentum L. We now do perturbation theory in $\hat{V}'$. Since the term added to H_0 is a pure (g-dependent) number, it will not change the energy denominators. However, the last term in Eq. (3.2) will now be absent. In the following we will assume that this has been done and drop the primes and the term involving the first-order energy in the third-order formula.

Second-order perturbation theory is equally straightforward:

$$E^{(2)}_{N+n}=\sum_{\beta}^{\text{ex}}\sum_{a,b}^{\text{occ}}\frac{|\langle a,b|\hat{V}|\beta\rangle|^2}{E^{(0)}-E^{(0)}(\beta)}\ ,\quad n=0,1\ , \tag{3.6}$$

$$E^{(2)}_{N+2}(m,m')=\sum_{\beta}\sum_{a,b}^{\text{occ}(m)}\sum_{a',b'}^{\text{occ}(m')}\frac{\langle a,b|\hat{V}|\beta\rangle\langle\beta|\hat{V}|a',b'\rangle}{E^{(0)}-E^{(0)}(\beta)}\ .$$

The summation over the numerous excited states $|\beta\rangle$ involves tedious bookkeeping of multiplicity factors, signs, and blocking of excitations by the conduction electrons. β enumerates states with electrons and holes. We are interested, however, primarily in the *pair energy* Δ of Eq. (1.1). A large number of "core excitations" present in (2.9) and (2.10) are unimportant since they cancel out in Δ. In the next section, we shall describe a diagrammatic method to compute Δ directly without the core excitations. This method provides us with a substantial reduction in computation time, as well as an independent check on our numerical calculations of E_{N+n}.

IV. DIAGRAMMATIC CALCULATION OF Δ

In this section we outline the procedure for a direct calculation of the pair energy Δ:

$$\begin{aligned}\Delta&=E_{N+2}(g)-2E_{N+1}(g)+E_N(g)\\&=g^{(1)}+g^2\Delta^{(2)}+\cdots\ ,\end{aligned} \tag{4.1}$$

where $N=2l_c^2$ is the number of electrons in the filled shells. We define the perturbation operator of order k,

$$\hat{U}^k=\hat{V}\left[\frac{1-\mathcal{P}_0}{E^{(0)}-H_0}\hat{V}\right]^{k-1}\ , \tag{4.2}$$

and consider its matrix elements between the states $|\Phi^m_n\rangle$, for $n=0,1,2$. Henceforth, we define $\langle A\rangle=\langle N|A|N\rangle$. For $n=0,1,2$, we have

$$U_0=\langle\hat{U}\rangle\ , \tag{4.3a}$$

$$\begin{aligned}U_1&=\langle c_{l_c m\uparrow}\hat{U}c^{\dagger}_{l_m\uparrow}\rangle\\&=\langle\{c_{l_c m\uparrow},[\hat{U},c^{\dagger}_{l_c m\uparrow}]\}\rangle+U_0\ ,\end{aligned} \tag{4.3b}$$

$$\begin{aligned}U_2(m,m')&=\langle c_{l_c m\uparrow}c_{l_c -m\downarrow}\hat{U}c^{\dagger}_{l_c -m'\downarrow}c^{\dagger}_{l_c m'\uparrow}\rangle\\&=\langle\{c_{l_c m\uparrow},[\{c_{l_c -m\downarrow}[\hat{U},c^{\dagger}_{l_c -m'\downarrow}]\},c^{\dagger}_{l_c m'\uparrow}]\}\rangle-\delta_{mm'}(2U_1-U_0)\ ,\end{aligned} \tag{4.3c}$$

where $[,]$ and $\{,\}$ are commutators and anticommutators, respectively. By (4.2) we see that the pair energy is given by

$$g^k\Delta^{(k)}(m,m')=\langle\{c_{l_c m\uparrow},[\{c_{-l_c m\downarrow}[\hat{U}^{(k)},c^{\dagger}_{-l_c m'\downarrow}]\},c^{\dagger}_{l_c m'\uparrow}]\}\rangle\ . \tag{4.4}$$

The successive commutation and anticommutation of $c^{\dagger}$'s and c's with $\hat{U}$ contracts four operators with the conduction electrons. The first-order perturbation operator $\hat{U}^{(1)}=\hat{V}$ has four fermion operators, which are removed in (4.4). There are no internal fermion contractions in $\Delta^{(1)}$,

$$\Delta^{(1)}(m,m')=\frac{1}{g}v_{l_c m l_c -m l_c m' l_c -m'}\ , \tag{4.5}$$

where v is defined in Eq. (2.12). Equation (4.5) is described by the first diagram of Fig. 3(b).

The higher-order terms include powers of the operator

$$\Pi_0=\frac{1-\mathcal{P}_0}{E^{(0)}-H_0}\ . \tag{4.6}$$

It is convenient to shift the zero for the single-particle energies to the conduction shell l_c:

$$\varepsilon_l=e_0[l(l+1)-l_c(l_c+1)]\ . \tag{4.7}$$

The shift of $-e_0 l_c(l_c+1)$ does not affect, of course, the energy denominators of Π_0. Using Eqs. (4.6) and (4.7), we find that

$$\begin{aligned}[H_0,c_{l_c ms}]=0&\Longrightarrow[\Pi_0,c_{l_c ms}]=0\ ,\\&[\Pi_0,c^{\dagger}_{l_c ms}]=0\ .\end{aligned} \tag{4.8}$$

After the contractions with the conduction electrons in (4.4), we need to calculate expectation values such as

$$\langle c^{\dagger}c^{\dagger}c\Pi_0 c\rangle,\langle c^{\dagger}c\Pi_0 c^{\dagger}c\rangle,\langle c^{\dagger}c^{\dagger}\Pi_0 cc\rangle,\ldots\ . \tag{4.9}$$

The fermion operators can be contracted in pairs, and the operator Π_0 yields the energy denominators of the intermediate states. All the possible contractions are described by the diagrams of $\Delta^{(2)}$ in Fig. 3(b). The evaluation of these diagrams is given by the following rules.

(1) All possible connected directed (with arrows) diagrams are drawn. Angular momenta l are assigned to the fermion lines. The right-pointing lines are particles $l\geq l_c$, and left-pointing lines or self-interaction loops denote holes with $l<l_c$. The sum over fermion momenta is weighted by $1/(|\varepsilon_l|+|\varepsilon_{l'}|)$, where ε_l are the particle or hole energies given by (4.7). The self-interaction loops do not contribute to this energy denominator.

(2) Each vertex contributes a factor of $(-1)^{\sum_i m_i}C^{Ll l'}_{Mm-m'}$, where m_i are the incoming momenta

to the vertex.

(3) Each interaction line of momentum L carries a factor of $2\pi r_{\min}[2/r_{\min}(2L+1)]^{\alpha}$, and there is a summation L.

(4) The diagrams are added to their three reflected counterparts given by replacing the external momenta: $(m,m')\rightarrow(-m,-m')$ and $(m,m')\rightarrow(m',m)$. The symmetry factor S is the number of inequivalent diagrams generated by this symmetrization. Te overall multiplicity factor is the product of S times the number of internal spin summations.

(5) The overall sign of a diagram is determined by signs of the fermion permutations. We start from Eq. (4.3) and permute each particle (hole) creation operator to the immediate right (left) of its contracted counterpart.

There are no blocking effects to be considered between different fermion lines since blocked processes of one diagram are compensated by blocked processes of another diagram with an opposite sign. Each diagram $d_i^{(k)}$ is separately rotationally invariant. This is checked by diagonalizing it with the Clebsch-Gordan transformation

$$d^{(k)}(L)=\sum_{m,m'}(L0|l_c-m,l_cm)d^{(k)}(m,m') \times(l_cm'l_c-m'|0L)\ . \tag{4.10}$$

The pair energy coefficients thus given by

$$\Delta^{(k)}(L)=\sum_i d_i^{(k)}(L)\ . \tag{4.11}$$

Similar diagrams to the above were previously used by Iwata and Freed[8] and by Brandow[9] to calculate effective Hamiltonians for π electrons in organic molecules. It is interesting to mention that Iwata and Freed were motivated by the apparent *reduction* of the triplet to singlet splitting by second-order polarization processes, a precursor effect to the pair-binding mechanism.

V. ESTIMATE OF THIRD ORDER AND g^{pert}

We will now examine the validity of truncating the perturbations series at second order. From Eq. (3.2) it is apparent that $E^{(1)}$ is qualitatively different from the higher-order corrections $E^{(k)}$, $k\geq 2$. The latter involve summations over excited states and energy denominators. Thus the magnitude of $g^{\text{pair}}=\Delta^{(1)}/\Delta^{(2)}$ could be quite different than the value of g^{pert} at which the third-order corrections become equal in magnitude to the second-order term:[10]

$$g^{\text{pert}}=|E^{(2)}/E^{(3)}|\ . \tag{5.1}$$

To estimate g^{pert} we first evaluate the weighted average over excited states of the interaction matrix elements. There are two distinct types of matrix elements $\langle\alpha|\hat{V}|\beta\rangle$ in the perturbation sums: types 1 and 2. Type 1 involves changes in one electron's state, and type 2 involves changes in the states of two electrons. The corresponding matrix elements (these are actually matrix elements of $\hat{V}'$ [Eq. (3.5)]) are

$$V_1=\sum_b^{\text{occ}(m)}\langle a,b|V|a',b\rangle\ , \qquad V_2=\langle a,b|V|a',b'\rangle\ , \tag{5.2}$$

where the summation in V_1 is over occupied states in the relevant ground state Φ_n^m. We define the weighted averages of the V_1 and V_2 matrix elements separately:

$$M_1=\overline{|V_1|(2L_{\min}+1)^{\alpha}}\ , \qquad M_2=\overline{|V_2|(2L_{\min}+1)^{\alpha}}\ , \tag{5.3}$$

where $L_{\min}$ is the minimal L which connects the angular momenta of the initial and final states and

$$\overline{\{\hat{A}\}}\equiv\frac{\sum_{a,b}^{\text{occ}}\sum_{a',b'}^{\text{unocc}}|\langle a,b|A|a',b'\rangle|}{\sum_{a,b}^{\text{occ}}\sum_{a',b'}^{\text{unocc}}}\ . \tag{5.4}$$

Our main assumption is that the matrix elements M_i, $i=1,2$, do not depend strongly on a,b,a',b' except through the factor $(2L_{\min}+1)^{-\alpha}$. This approximation is justified by the insensitivity of the values of M_i to the parameter α.

Using this assumption, we can approximate the magnitudes of the second- and third-order energies. The second-order energy can be written as

$$E^{(2)}=\sum_{i=1}^{2}E_i^{(2)}\ , \tag{5.5a}$$

$$E_i^{(2)}=M_i^2S_i\ , \tag{5.5b}$$

$$S_1=\sum_{l=0}^{l_s}\sum_{l'=l_c}^{l_{\max}}\frac{2(2l+1)}{[2(l'-l)+1]^{2\alpha}(\varepsilon_{l'}-\varepsilon_l)}\ , \tag{5.5c}$$

$$S_2=\sum_{l_1\leq l_2=0}^{l_s}\sum_{l'\leq l''=l_c}^{l_{\max}}\frac{6(2l_1+1)(2l_2+1)(2l'+1)}{[2(l'-l_1)+1]^{2\alpha}(\varepsilon_{l'}+\varepsilon_{l''}-\varepsilon_{l_1}-\varepsilon_{l_2})}\ , \tag{5.5d}$$

where ε_l is the zeroth-order energy of l,m of Eq. (2.2). The weight factors S_1 and S_2 include the energy denominators of the one- and two-particle excitations, respectively. The values of $E_i^{(2)}$ are computed exactly, which together with the values of S_i yields the averaged matrix elements

$$M_i = \left[\frac{E_i^{(2)}}{S_i} \right]^{1/2} . \tag{5.6}$$

The third-order energies are estimated using the matrix elements given by (5.6) and (3.2):

$$E^{(3)} \simeq \sum_{i,j,k=1,2} M_i M_j M_k S_{ijk} - E^{(1)} F^{(3)} ,$$
$$F^{(3)} = g^{-2} \sum_{\beta}^{\text{occ}} \sum_{a,b}^{\text{occ}} \sum_{a',b'} \frac{\langle a,b|\hat{V}|\beta\rangle\langle\beta|\hat{V}|a',b'\rangle}{[E^{(0)} - E^{(0)}(\beta)]^2} , \tag{5.7}$$

where (ijk) represents allowed sequences of one- and two-particle transitions participating in the third-order sums. Explicit formulas for S_{ijk} are given in the Appendix. The estimate for $E^{(3)}$ is probably an *overestimate,* since it ignores relative sign cancellations. We have verified that, for various l_c and $l_{\max}$, M is weakly dependent on α, which justifies this procedure.

VI. RESULTS

In Fig. 4, $\Delta(L)$ for $\alpha=0.2$, $l_c=5$, and $l_{\max}=6$ is plotted as a function of g. This system has 50 closed-shell electrons and 98 available states in the Hilbert space. The ratio of occupied to unoccupied states resembles the corresponding ratio in the Hubbard model of C_{60}. The $n=2$ system has 11 multiplets in its ground-state manifold with $0 \le L \le 10$. The first-order coefficients $\Delta^{(1)}$ are always non-negative. The singlet ($L=0$, $S=0$) state is initially the highest state in the multiplet, and the ($L=7$, $S=1$) is the lowest. This is a weak violation of Hund's rule, which would predict ($L=9$, $S=1$) to be the lowest state. Because of Pauli's principle, for the δ-function potential ($\alpha=0$), the odd-L coefficients vanish, $\Delta^{(1)}(L)=0$, $L=1,3,5,7,9$.

The results for the second-order coefficients $\Delta^{(2)}(L)$ are less predictable. The polarization of the closed-shell electrons enters at this order. Negative Δ implies that the two electrons prefer to share that polarization. For all $l_c \le 6$, $l_{\max} \le 7$, and α, we have found the $\Delta^{(2)}(0)$k is always negative and largest in magnitude. Second-order perturbation theory implies that there would be level crossings, and at some g the $L=0$ singlet would become the ground state, as seen in Fig. 4. At

$$g^{\text{pair}}(0) = -\Delta^{(1)}(0)/\Delta^{(2)}(0) , \tag{6.1}$$

the singlet pair-binding energy becomes negative.

We also find that $\Delta^{(2)}(L=1)<0$ for the range of filling parameters $4 \le l_c \le l_{\max} \le 8$. For the δ-function potential, since $\Delta^{(1)}(1)=0$, this negativity implies that *triplet pairing is possible in the $L=1$ channel for arbitrary small g.* This effect clearly survives the higher-order corrections. In Fig. 5 the ground-state phase diagram in g,α space is shown.

The values of g^{pert} are plotted in Figs. 4 and 5 by dot-dashed lines. For $g \ll g^{\text{pert}}$ the results of second-order perturbation theory are expected to hold. We note that the exact solution of the two- to four-electron system with $l_c = l_{\max} = 1$ has no pair binding.[11] For that system $g^{\text{pair}} = 16\pi$ is larger than $g^{\text{pert}} \approx 15$ by a factor of 3. This indicates correctly that second-order results are not expected to hold. We expect that for a larger number of electrons our procedure for estimating the third-order matrix elements works even better.

In general, we have found that g^{pair} ($L=0$) and g^{pert} decrease as the cutoff momentum $l_{\max}$ increases, although g^{pert} decreases faster. On the other hand, $g^{\text{pair}}(L=1)$ in-

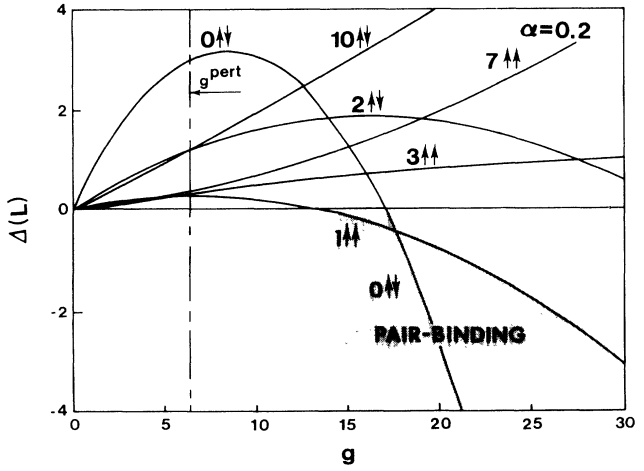

FIG. 4. Second-order approximation for the pair-binding energies (in units of e_0) of several angular-momentum channels. $\uparrow\downarrow$ and $\uparrow\uparrow$ denote spin singlet and triplet, respectively. The pair-binding region is shaded. Left of g^{pert} (dot-dashed line), higher-order corrections are expected to be small. Here $l_c=5$, $l_{\max}=6$, and $\alpha=0.2$ (see text for definitions).

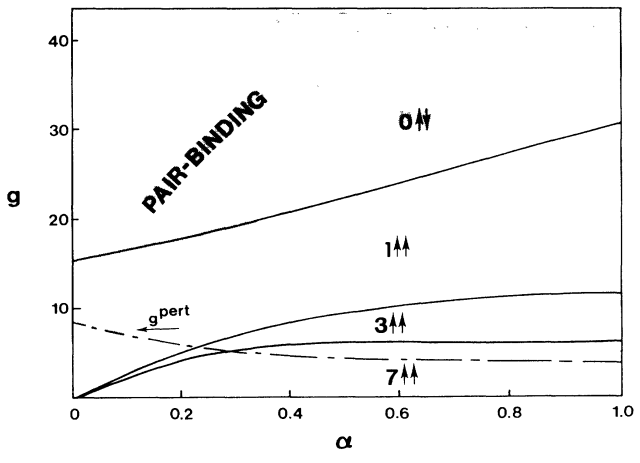

FIG. 5. Second-order prediction for the ground-state phase diagram of the $l_c=5$, $l_{\max}=6$ system. g and α describe the strength and range of the interaction, respectively. Smaller α corresponds to shorter-range interactions. The shaded region represents pair binding. Below g^{pert} (dot-dashed line), higher-order corrections are expected to be small.

creases with l_{max}. We have not yet included the lattice potential or different electron fillings. By comparing our results to CK's Hubbard model, we learn that the singlet pair binding is robust, while the triplet pair binding does not survive the lattice potential in the tight-binding limit. Their results also suggest that the pair-binding energy is insensitive to the precise filling of the $L=5$ multiplet.

To emulate the C_{60} molecule with our model, we use $R=3.5$ Å, the bare electron mass, a dielectric constant of unity to obtain $e_0=0.242$ eV, and a bare interaction parameter $g_0=8.4$. It is heartening to realize that g_0 is situated in a physically interesting regime of Fig. 5, for sufficiently screened interactions (small α). The effective g depends on the effective mass and short-distance dielectric constant. The precise value of α is difficult to estimate for X_3C_{60}. It depends on the detailed polarization of the other degrees of freedom on the system, including phonons, σ, and core electrons. In addition, the effects of neighboring atoms in the crystal are very important.

In summary, we can now answer the three questions posed earlier: (i) The lattice is not essential for pair binding. (ii) Longer-range interactions (larger α) push g^{pair} to higher values, where the second-order results are less reliable. (iii) One can trust the second-order results for the pair-binding energies in the regime $g \ll g^{\text{pert}}$.

VII. SUPERCONDUCTIVITY IN X_3C_{60}

Although our second-order results for pair-binding energy $|\Delta|$ in the *singlet* channel are not conclusive, it is worth discussing its implication on the ground state of the full molecular crystal. We consider the negative-U Hubbard model on an fcc lattice of C_{60} molecules:

$$H^{X_3C_{60}}=-t\sum_{s(nn')}^{\text{fcc}} b_{ns}^{\dagger}b_{n's}-|\Delta|\sum_{n}(n_{n\uparrow}-\tfrac{1}{2})(n_{n\downarrow}-\tfrac{1}{2}) , \tag{7.1}$$

where (nn') are nearest neighbors on the fcc lattice, $b_{ns}^{\dagger}$ creates an electron of spin s at the nth C_{60} site, and t is the intermolecular hopping energy. The alakali-metal atoms donate one electron each. Their hybridization with the C_{60} molecules determines t.

There are two opposite limits where (7.1) can be solved: the weak-coupling limit ($|\Delta|/t \ll 1$) and the strong-coupling limit $|\Delta|/t \gg 1$. Chakravarty and Kivelson [2] have shown that superconductivity arises in the weak-coupling regime. By the pressure dependence of the transition temperature, they argue that the physical superconductors are in this regime. Here we show that superconductivity arises *also in the strong-coupling regime.* We make use of a straightforward mapping of (7.1) to a magnetic model. First, we transform (7.1) by defining

$$\begin{aligned} b_{n\downarrow}^{\dagger}&=\tilde{b}_{n\downarrow} ,\\ b_{n\uparrow}^{\dagger}&=\tilde{b}_{n\uparrow}^{\dagger} . \end{aligned} \tag{7.2}$$

The transformed Hamiltonian is the model

$$\tilde{H}=-t\sum_{s(nn')}^{\text{fcc}}(\tilde{b}_{n\uparrow}^{\dagger}\tilde{b}_{n'\uparrow}-\tilde{b}_{n\downarrow}^{\dagger}\tilde{b}_{n'\downarrow}) +|\Delta|\sum_{n}(\tilde{n}_{n\uparrow}-\tfrac{1}{2})(\tilde{n}_{n\downarrow}-\tfrac{1}{2}) . \tag{7.3}$$

For large $|\Delta|/t \gg 1$, (7.3) can be transformed by second-order perturbation theory in $t/|\Delta|$ into the spin model

$$\tilde{H}\rightarrow\frac{2t^2}{\Delta}\sum_{s(nn')}^{\text{fcc}}(\tilde{S}_n^z\tilde{S}_{n'}^z-\tilde{S}_n^x\tilde{S}_{n'}^x-\tilde{S}_n^y\tilde{S}_{n'}^y+\tfrac{1}{4}\tilde{n}_n\tilde{n}_{n'}) +O(t^3/|\Delta|^2)+\cdots , \tag{7.4}$$

where $\tilde{n}=\sum_s\tilde{b}_s^{\dagger}\tilde{b}_s$ is the local density and $(\tilde{S}^x,\tilde{S}^y,\tilde{S}^z)$ are spin-$\frac{1}{2}$ operators defined by

$$\tilde{S}_n^z=n_n-\tfrac{1}{2} , \quad \tilde{S}_n^x+i\tilde{S}_n^y=b_{n\uparrow}^{\dagger}b_{n\downarrow}^{\dagger} , \tag{7.5}$$

and therefore ordering of (7.4) in the xy plane $\langle S^+\rangle\neq 0$ implies superconductivity in the original model (7.1). Now, since the classical version of (7.4) on the fcc lattice is frustrated, it cannot satisfy all the antiferromagnetic bonds of $\tilde{S}_n^z\tilde{S}_{n'}^z$. Thus the *classical* ground state is ordered ferromagnetically in the xy plane; i.e., we obtain a superconductor and not a charge-density-wave system. We expect the classical ground state to be a good zeroth-order approximation for the quantum ground state of Eq. (7.4) since the lattice is three dimensional.

For the case of pair binding in the triplet channel, in order to obtain superconductivity, we need to consider at least three orbitals per site. This calculation has not yet been done. Our guess is that for large $|\Delta|/t$ we would obtain a novel ferromagnetic superconductor similar to the superfluid phases of ^{3}He. The recent discovery of ferromagnetism in tetrakis(dimethylamine)ethylene-C_{60} (Ref. 12) indicates that the physical parameters of that system might not be forbiddingly far from achieving triplet pair binding.

ACKNOWLEDGMENTS

We thank S. Chakravarty and S. Kivelson for valuable discussions and the Aspen Center for Physics where parts of this work were done. This work has been supported in part by a grant from the NSF, No. DMR-8914045, and Grant No. 90-00441/1 from the U.S.-Israel Binational Science Foundation. A.A. acknowledges the Alfred P. Sloan Foundation for partial support.

APPENDIX: WEIGHT FACTORS OF THIRD-ORDER PERTURBATION THEORY

We have collected the formulas for the weight factors of third-order perturbation theory here for completeness. In third-order perturbation theory, there are three consecutive processes (ijk), where $i,j,k=1,2$. Processes of types 1 and 2 were defined before Eq. (5.2). A description of the process in terms of the intermediate states follows each formula. We use Latin indices for labeling the positions of holes and Greek indices for particles. As in Sec. V, ε_l stands for the zeroth-order energy of state l,m of Eq. (2.2):

$$S_{111}=\sum_{l-0}^{l_s}\sum_{\lambda_1\neq\lambda_2=l_c}^{l_{\max}}\frac{2(2l+1)}{\{[2(\lambda_1-l)+1][2(\lambda_2-l)+1](2|\lambda_1-\lambda_2|+1)\}^{\alpha}}\frac{1}{(\varepsilon_{\lambda_1}-\varepsilon_l)(\varepsilon_{\lambda_2}-\varepsilon_l)}$$
$$+\sum_{l,l'=0}^{l_s}\sum_{\lambda=l_c}^{l_{\max}}\frac{2(2l+1)}{\{[2(\lambda-1)+1][2(\lambda-l')+1](2|l-l'|+1)\}^{\alpha}}\frac{1}{(\varepsilon_{\lambda}-\varepsilon_l)(\varepsilon_{\lambda}-\varepsilon_{l'})}\ . \tag{A1}$$

The first sum represents the process $|0\rangle\rightarrow|l,\lambda_1\rangle\rightarrow|l,\lambda_2\rangle\rightarrow|0\rangle$, whereas the second sum represents the process $|0\rangle\rightarrow|l_1,\lambda\rangle\rightarrow|l_2,\lambda\rangle\rightarrow|0\rangle$.

$$S_{112+211}=\sum_{l_1,l_2=0}^{l_s}\sum_{\lambda_1,\lambda_2=l_c}^{l_{\max}}\frac{8(2l_1+1)(2l_2+1)}{\{[2(\lambda_1-l_1)+1][2(\lambda_2-l_2)+1][2(\lambda_{\min}-l_{\max})+1]\}^{\alpha}}\frac{1}{(\varepsilon_{\lambda_1}-\varepsilon_{l_1})(\varepsilon_{\lambda_1}+\varepsilon_{\lambda_2}-\varepsilon_{l_1}-\varepsilon_{l_2})}\ . \tag{A2}$$

This represents the process $|0\rangle\rightarrow|l_1,\lambda_1\rangle->|l_1,\lambda_1,l_2,\lambda_2\rangle\rightarrow|0\rangle$.

$$S_{121}=\sum_{l_1,l_2=0}^{l_s}\sum_{\lambda_1,\lambda_2=l_c}^{\lambda_{\text{cut}}}\frac{8(2l_1+1)(2l_2+1)}{\{[2(\lambda_1-l_1)+1][2(\lambda_2-l_2)+1][2(\lambda_{\min}-l_{\max})+1]\}^{\alpha}}\frac{1}{(\varepsilon_{\lambda_1}-\varepsilon_{l_1})(\varepsilon_{\lambda_2}-\varepsilon_{l_2})}\ . \tag{A3}$$

This represents the process $|0\rangle\rightarrow|l_1,\lambda_1\rangle\rightarrow|l_2,\lambda_2\rangle\rightarrow|0\rangle$.

$$S_{122+221}=\sum_{l_1,l_2=0}^{l_s}\sum_{\lambda_1,\lambda_2,\nu=l_c}^{l_{\max}}\frac{8(2l_1+1)(2l_2+1)[2\min(\lambda_2,\nu)+1]}{(\varepsilon_{\lambda_1}-\varepsilon_{l_1})(\varepsilon_{\lambda_2}+\varepsilon_{\nu}-\varepsilon_{l_1}-\varepsilon_{l_2})}$$
$$\times\frac{1}{([2(\lambda_1-l_1)+1][2|\min(\lambda_2,\nu)-\lambda_1|+1]\{2[\min(\lambda_2,\nu)-l_{\min}]+1\})^{\alpha}}$$
$$+\sum_{l_1=0}^{l_s}\sum_{l_2\geq l_3=0}^{l_s}\sum_{\lambda_1,\lambda_2=l_c}^{l_{\max}}\frac{12(2l_1+1)(2l_2+1)(2l_3+1)}{\{[2(\lambda_1-l_1)+1][2(\lambda_2-l_3)+1][2(\lambda_{\min}-l_3)+1]\}^{\alpha}}$$
$$\times\frac{1}{(\varepsilon_{\lambda_1}-\varepsilon_{l_1})(\varepsilon_{\lambda_1}+\varepsilon_{\lambda_2}-\varepsilon_{l_3}-\varepsilon_{l_2})}\ . \tag{A4}$$

Here the first sum represents $|0\rangle\rightarrow|l_1,\lambda_1\rangle\rightarrow|l_1,l_2,\lambda_2,\nu\rangle\rightarrow|0\rangle$ and the second sum represents $|0\rangle\rightarrow|l_1,\lambda_2\rangle\rightarrow|l_3,l_2,\lambda_1,\lambda_2\rangle\rightarrow|0\rangle$.

$$S_{212}=\sum_{l_1\leq l_2=0}^{l_s}\sum_{\lambda_1\leq\lambda_2=l_c}^{l_{\max}}\sum_{\nu=l_c}^{l_{\max}}\frac{6(2l_1+1)(2l_2+1)(2\lambda_1+1)}{([2(\lambda_1-l_1)+1](2|\lambda_2-\nu|+1)\{2[\min(\lambda_1,\nu)-l_1]+1\})^{\alpha}}$$
$$\times\frac{1}{(\varepsilon_{\lambda_1}+\varepsilon_{\lambda_2}-\varepsilon_{l_1}-\varepsilon_{l_2})(\varepsilon_{\lambda_1}+\varepsilon_{\nu}-\varepsilon_{l_1}-\varepsilon_{l_2})}+(\lambda_1\leftrightarrow\lambda_2)$$
$$+\sum_{l_1\leq l_2=0}^{l_s}\sum_{l_3=0}^{l_s}\sum_{\lambda_1\leq\lambda_2=l_c}^{l_{\max}}\frac{6(2l_1+1)(2l_2+1)(2\lambda_1+1)}{([2(\lambda_1-l_1)+1](2|l_3-l_1|+1)\{2[\lambda_1-\min(l_2,l_3)]+1\})^{\alpha}}$$
$$\times\frac{1}{(\varepsilon_{\lambda_1}+\varepsilon_{\lambda_2}-\varepsilon_{l_1}-\varepsilon_{l_2})(\varepsilon_{\lambda_1}+\varepsilon_{\lambda_2}-\varepsilon_{l_2}-\varepsilon_{l_3})}+(l_1\leftrightarrow l_2)\ . \tag{A5}$$

Here the four sums represent the processes

$$|0\rangle\rightarrow|l_1,l_2,\lambda_1,\lambda_2\rangle\rightarrow|l_1,l_2,\lambda_1,\nu\rangle\rightarrow|0\rangle\ ,$$
$$|0\rangle\rightarrow|l_1,l_2,\lambda_1,\lambda_2\rangle\rightarrow|l_1,l_2,\lambda_2,\nu\rangle\rightarrow|0\rangle\ , \tag{A6}$$
$$|0\rangle\rightarrow|l_1,l_2,\lambda_1,\lambda_2\rangle\rightarrow|l_2,l_3,\lambda_1,\lambda_2\rangle\rightarrow|0\rangle\ ,$$

and

$$|0\rangle\rightarrow|l_1,l_2,\lambda_1,\lambda_2\rangle\rightarrow|l_1,l_3,\lambda_1,\lambda_2\rangle\rightarrow|0\rangle\ ,$$

respectively.

$$
\begin{aligned}
S_{222}=&\sum_{l_1\le l_2=0}^{l_s}\sum_{\lambda_1\le\lambda_2=l_c}^{l_{\max}}\sum_{\nu_1\le\nu_2=l_c}^{l_{\max}}\frac{9(2l_1+1)(2l_2+1)(2\lambda_1+1)(2\nu_1+1)}{\{[2(\lambda_1-l_2)+1](2|\nu_1-\lambda_2|+1)[2(\lambda_1-l_2)+1]\}^{\alpha}}\\
&\times\frac{1}{(\varepsilon_{\lambda_1}+\varepsilon_{\lambda_2}-\varepsilon_{l_1}-\varepsilon_{l_2})(\varepsilon_{\nu_1}+\varepsilon_{\nu_2}-\varepsilon_{l_1}-\varepsilon_{l_2})}\\
&+\sum_{l_1\le l_2=0}^{l_s}\sum_{\lambda_1\le\lambda_2=l_c}^{l_{\max}}\sum_{l_3=0}^{l_s}\sum_{\lambda_3=l_c}^{l_{\max}}\frac{6(2l_1+1)(2l_2+1)(2\lambda_1+1)(2l_3+1)}{(\varepsilon_{\lambda_1}+\varepsilon_{\lambda_2}-\varepsilon_{l_1}-\varepsilon_{l_2})(\varepsilon_{\lambda_1}+\varepsilon_{\lambda_3}-\varepsilon_{l_1}-\varepsilon_{l_3})}\\
&\times\frac{1}{([2(\lambda_1-l_1)+1](2|l_2-l_3|+1)\{2[\min(\lambda_1,\lambda_3)-\min(l_1,l_3)]+1\})^{\alpha}}\\
&+(l_1\leftrightarrow l_2)+(\lambda_1\leftrightarrow\lambda_2)+(l_1\leftrightarrow l_2,\lambda_1\leftrightarrow\lambda_2)\\
&+\sum_{l_1\le l_2=0}^{l_s}\sum_{l_3\le l_4=0}^{l_s}\sum_{\lambda_1\le\lambda_2=l_c}^{l_{\max}}\frac{9(2l_1+1)(2l_2+1)(2\lambda_1+1)(2l_3+1)}{\{[2(\lambda_1-l_1)+1](2|l_4-l_2|+1)[2(\lambda_1-l_3)+1]\}^{\alpha}}\\
&\times\frac{1}{(\varepsilon_{\lambda_1}+\varepsilon_{\lambda_2}-\varepsilon_{l_1}-\varepsilon_{l_2})(\varepsilon_{\lambda_1}+\varepsilon_{\lambda_2}-\varepsilon_{l_3}-\varepsilon_{l_4})}\ . \qquad \text{(A7)}
\end{aligned}
$$

Here the six terms represent the processes

$$
\begin{aligned}
&|0\rangle\to|l_1,l_2,\lambda_1,\lambda_2\rangle\to|l_1,l_2,\nu_1,\nu_2\rangle\to|0\rangle\ ,\\
&|0\rangle\to|l_1,l_2,\lambda_1,\lambda_2\rangle\to|l_1,l_3,\lambda_1,\lambda_3\rangle\to|0\rangle\ ,\\
&|0\rangle\to|l_1,l_2,\lambda_1,\lambda_2\rangle\to|l_2,l_3,\lambda_1,\lambda_3\rangle\to|0\rangle\ ,\\
&|0\rangle\to|l_1,l_2,\lambda_1,\lambda_2\rangle\to|l_1,l_3,\lambda_2,\lambda_3\rangle\to|0\rangle\ ,\\
&|0\rangle\to|l_1,l_2,\lambda_1,\lambda_2\rangle\to|l_2,l_3,\lambda_2,\lambda_3\rangle\to|0\rangle\ ,
\end{aligned}
\qquad \text{(A8)}
$$

and

$$
|0\rangle\to|l_1,l_2,\lambda_1,\lambda_2\rangle\to|l_3,l_4,\lambda_1,\lambda_2\rangle\to|0\rangle\ ,
$$

respectively. Note that we are considering a sum of positive terms. In reality, third-order contributions will come with different signs, so that the above is most probably an overestimate. We cannot make it a rigorous bound because we are using the averaged matrix elements. We must emphasize that this is an order-of-magnitude estimate only and must be accepted as a rough guideline for determining if second-order perturbation theory is reliable.

[1]A. F. Hebard, M. J. Rosseinsky, R. C. Haddon, D. W. Murphy, S. H. Glarum, T. T. M. Palstra, A. P. Ramirez, and A. R. Kortran, Nature (London) **350**, 600 (1991); K. Holczer, O. Klein, G. Gruner, S.-M. Huang, R. B. Kaner, K.-J. Fu, R. L. Whetten, and F. Diedrich, Science **252**, 1154 (1991).

[2]S. Chakravarty and S. Kivelson, Europhys. Lett. **16**, 751 (1991); S. Chakravarty, M. P. Gelfand, and S. Kivelson, Science **254**, 970 (1991); S. White, S. Chakravarty, M. P. Gelfand, and S. Kivelson, Phys. Rev. B **45**, 5062 (1992).

[3]Here the pair-binding energy Δ is opposite in sign to the definition of Ref. 2.

[4]Y. Hasegawa and D. Poilblanc, Phys. Rev. B **40**, 9035 (1989); R. M. Fye, M. J. Martins, and R. J. Scalettar, *ibid.* **42**, 6800 (1990); E. Dagotto, A. Moreo, F. Ortolani, D. Poilblanc, J. Riera, and D. Scalapino (unpublished); S. R. White (unpublished).

[5]Assa Auerbach and Ganpathy N. Murthy (unpublished).

[6]E. Manousakis, Phys. Rev. B **44**, 10 991 (1991).

[7]A. R. Edmonds, *Angular Momentum in Quantum Mechanics* (Princeton University, Princeton, NJ, 1974), p. 63.

[8]S. Iwata and K. F. Freed, J. Chem. Phys. **61**, 1500 (1974); **65**, 1071 (1976). These authors were motivated by the apparent *reduction* of the triplet to singlet splitting by second-order polarization processes; an effect similar to the pair-binding mechanism.

[9]B. H. Brandow, Int. J. Quantum Chem. **15**, 207 (1979).

[10]We are indebted to Steve Kivelson for bringing this fact to our attention.

[11]Assa Auerbach and Ganpathy N. Murthy (unpublished).

[12]P.-M. Allemand, K. C. Khemani, A. Koch, F. Wudl, K. Holczer, S. Donovan, G. Gruner, and J. D. Thompson, Science **253**, 301 (1991).

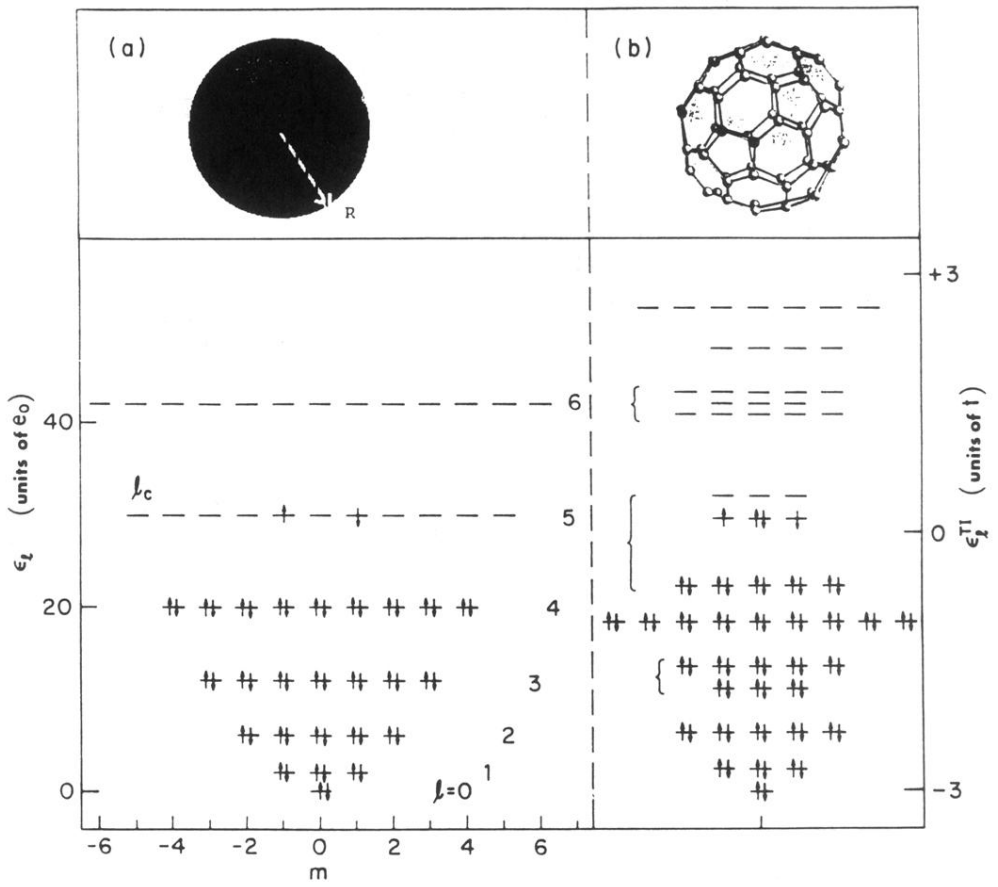

FIG. 1. (a) Spectra of noninteracting electrons on a sphere [Eq. (2.2)] with $l_c=5$ and $l_{max}=6$. We show the occupied states in one of the degenerate ground states of the 52-electron system. (b) The spectrum of the noninteracting tight-binding model (Ref. 6) on the truncated icosahedron (TI) lattice [Eq. (2.3)]. The lattice is depicted on top. The occupied states of a 63-electron ground state are shown.

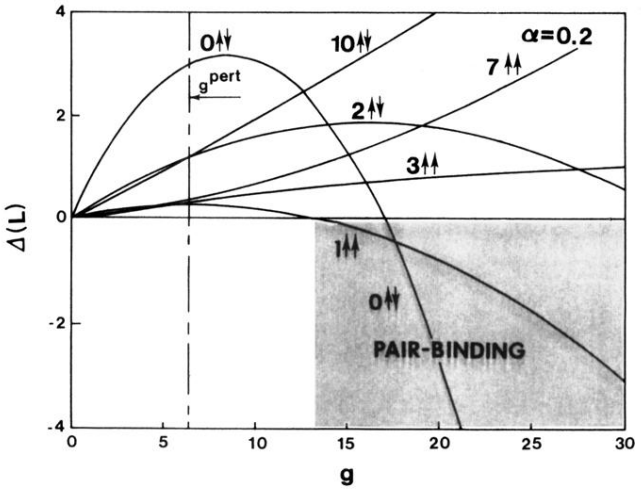

FIG. 4. Second-order approximation for the pair-binding energies (in units of e_0) of several angular-momentum channels. $\uparrow\downarrow$ and $\uparrow\uparrow$ denote spin singlet and triplet, respectively. The pair-binding region is shaded. Left of g^{pert} (dot-dashed line), higher-order corrections are expected to be small. Here $l_c=5$, $l_{\max}=6$, and $\alpha=0.2$ (see text for definitions).

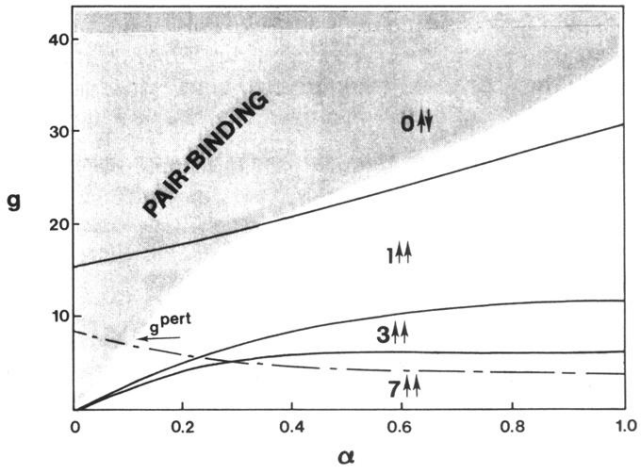

FIG. 5. Second-order prediction for the ground-state phase diagram of the $l_c=5$, $l_{max}=6$ system. g and α describe the strength and range of the interaction, respectively. Smaller α corresponds to shorter-range interactions. The shaded region represents pair binding. Below g^{pert} (dot-dashed line), higher-order corrections are expected to be small.